Моніторинг і контроль систем твердооксидних паливних елементів (ТОПЕ) в режимі реального часу мають важливе значення для визначення та розуміння продуктивності комірок. Деякі параметри, що впливають на продуктивність комірок ТОПЕ, включають витрату пального, температуру печі і сам матеріал комірок. Ці параметри взаємопов'язані при створенні комірок ТОПЕ, які застосовуються в якості джерела альтернативної енергії. Це дозволяє отримати надійні комірки ТОПЕ, оптимальну вихідну напругу і нижчу робочу температуру. Оскільки досі матеріалом комірок ТОПЕ є кераміка, робоча температура якої становить від 500 до 1000 °С. Моніторинг обмежений робочим середовищем ТОПЕ навколо печі. Робота ТОПЕ обмежена каналами подачі водню і кисню. Максимальна робоча температура печі складає 1000 градусів, а мінімальна вихідна напруга для однієї комірки. Тому необхідно розмістити чутливі точки датчика в міру необхідності. Метою даного дослідження є розробка системи моніторингу та регулювання потоку водню/кисню в робочому середовищі ТОПЕ на основі мікроконтролера Arduino Mega 2560 і комп ютерного інтерфейсу. Управління клапанами здійснюється за допомогою методів управління в розімкнутому контурі і двопозиційного управління. Управління в розімкнутому контурі використовується для установки значення кута повороту клапана. Двопозиц йне управл ня використовується для автоматичного закриття клапана при наявності надлишкової концентрації водню в лабораторному приміщенні. Система призначена для проведення лабораторних експериментів на простих печах. Цей пристрій також функціонує як простий міні-зразок. Тому його можна використовувати в якості матеріалу для широкого вивчення системи ТОПЕ. Результати випробувань зразка показують, що витрату водню можна регулювати від 0,07 до 4,74 л/хв, а кисню – від 0,24 до 4,8 л/хв. Датчики температури мають середню похибку 2,6 %, а датчики напруги – 0,1 В

Ключові слова: ТОПЕ, водень, кисень, продуктивність, комірка, датчик, витрата, ардуіно, напруга, піч

UDC 620.92
DOI: 10.15587/1729-4061.2020.194852

EXPERIMENTAL SET-UP DESIGN OF SOFC SINGLE CELL PERFORMANCE USING SIMPLE FURNACE WITH MAXIMUM TEMPERATURE OF 1000 DEGREES

Darjat
PhD, Associate Professor*
E-mail: dr.darjat@gmail.com
Sulistyo
Doctor of Technical Sciences, Associate Professor
Department of Mechanical Engineering**
E-mail: listyo2007@gmail.com
Aris Triwiyatno
Doctor of Technical Sciences, Associate Professor*
E-mail: aristriwiyatno@yahoo.com
Sumardi
PhD, Associate Professor*
E-mail: sumardi@elektro.undip.ac.id
Isroni Widiyantoro
PhD*
E-mail: rony.mfd@gmail.com
*Department of Electrical Engineering**
**Diponegoro University
Jalan. Prof. Sudarto, Tembalang,
Semarang, Indonesia, 50275

Received date 12.01.2020
Accepted date 07.02.2020
Published date 28.02.2020

1. Introduction

Solid oxide fuel cells (SOFC) have the potential to solve future energy needs. SOFC technology is environmentally friendly, clean-operation, quiet and high-efficiency. SOFC is an electrochemical cell that converts chemical energy into electrical energy by oxidizing its fuel and operating at temperatures of 600–1000 °C. This fuel cell has a high efficiency that can reach 65 %, the residual combustion is water (H_2O) and without pollutants [1–3].

Therefore, much research has focused on maximizing the performance of single cell stacks. At the stack level, several factors cause loss of performance due to the fragile nature of SOFC ceramics, the type of current collector, channel size and the mismatch of thermal expansion of stack components. However, the design of fuel/gas flow is one of the most significant factors affecting the performance of a single cell SOFC stack. In other words, the distribution of fuel/gas with the flow channel in the interconnection is one of the important parameters in the SOFC stack design. One model for viewing measurement performance and cell characteristics performed with an experimental set-up is illustrated in Fig. 1 [3].

Monitoring the direct surface temperature distribution of the SOFC system is important for identifying temperature-related degradation and understanding cell performance. This type of monitoring is limited to the SOFC operating

environment. SOFC operating temperature variations are generally predicted based on modeling that takes into account the conventional current-voltage curve. Temperature data obtained experimentally are very important for the management of high-temperature related degradation and for more reliable SOFC modeling. In this study, the distribution of SOFC temperatures was monitored in the place along the cell cathode simultaneously, using a commercial thermocouple. Fig. 2 illustrates the placement of a commercial thermocouple sensor on a cathode cell. Monitoring cell temperature and voltage is carried out through computer software [4].

An SOFC simulator study based on a microcontroller has been conducted. This research develops SOFC stack cell output voltage control to optimize the flow rate of fuel (hydrogen) and air (oxygen). The simulator is designed using the fuzzy logic control method. The controller can correct the SOFC output voltage and gas pressure difference below 8,106 Pa [5].

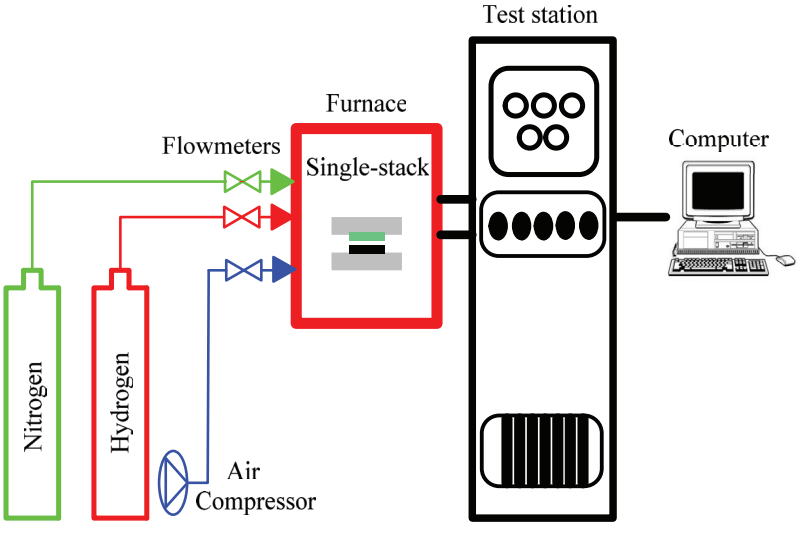

Fig. 1. Experimental set-up [3]

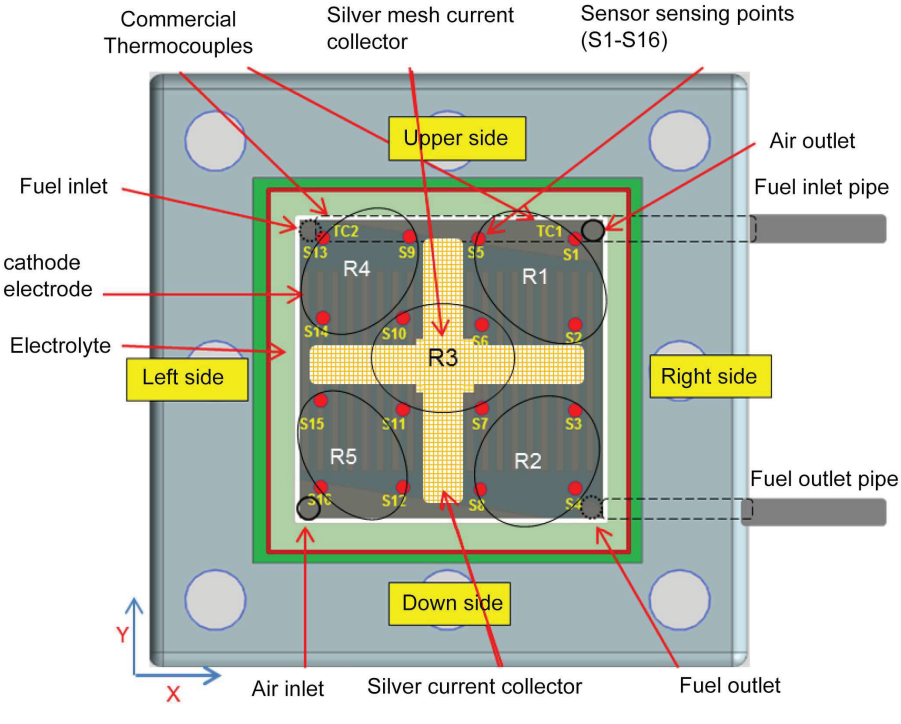

Fig. 2. Schematic placement of the thermocouple sensor at the cell cathode [4]

So far, there are no researchers who have made supporting devices for optimizing fuel/gas flow rates in a simple SOFC furnace with a maximum temperature of 1,000 degrees. This device is equipped with sensors that can see changes in measurement data. Large variations in gas flow can be adjusted from 0 to 5 L/min.

2. Literature review and problem statement

Today, with the restructuring of electricity utilities, technological evolution, public environmental policy, and expansion of power demand, expanding power demand provides opportunities for fuel cells to become important energy resources. Major improvements in the economic, operational and environmental performance of small modular units have been achieved through decades of intensive research. Among the distributed energy resources, microturbine and fuel cells show special expectations because they can operate on several fuels with low emissions, high efficiency, and high reliability [5]. Fuel cell technology is expected to substantially reduce oil dependency and environmental impact compared to conventional combustion-based power generation technology. Solid oxide fuel cells have the added advantage of high efficiency, the ability to utilize high-temperature exhaust for cogeneration or hybrid applications, and the ability for internal reform. SOFC is preferred for high power applications and is also recommended for distributed power and mobile assistive units. Alternative materials and manufacturing for solid oxide fuel cells are listed and analyzed. Specifically, the anode material category, the cathode material category, the electrolyte category, and the interconnect material category [7].

SOFC is an electrochemical reactor that can directly convert chemical energy from gas fuels into electrical energy with high efficiency and environmentally friendly. The latest trend in SOFC research concerns the use of available hydrocarbon fuels, such as natural gas. Fuel cells are devices for converting chemical energy from fuel to electrochemical electricity and heat without the need for direct combustion as an intermediary step, providing much higher conversion efficiency than traditional energy conversion systems. In addition, this technology does not produce large amounts of pollutants such as nitrogen oxides compared to internal combustion engines. As a result, fuel cells are seen as a more ideal source of energy in transportation, stationary, and distributed electricity generators [8].

SOFC has been present as an energy conversion device in achieving high efficiency of more than 70 % by

regeneration. The critical components of SOFC consist of anodes, electrolytes and cathodes. However, for the SOFC stack itself, the evaluation of seals and interconnections is also important. The SOFC stack has fuel (hydrogen) and air/oxygen inputs. The fuel input side has excess fuel and water drainage. Likewise for the air/oxygen also has an air outlet. Fig. 3 illustrates a stack of SOFC cells including fuel/air channels [9].

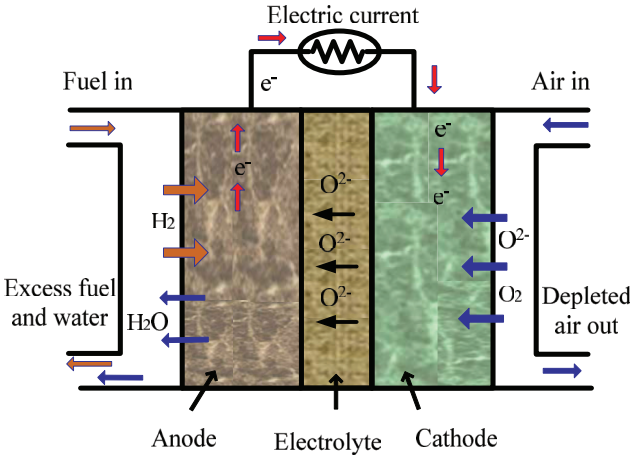

Fig. 3. Oxide-ion conducting electrolyte [9]

Fuel cell technology is considered a promising option for power generation in the current era of energy and security crises. Among various types of fuel cells, SOFC is considered as one of the promising alternatives for electricity generation because of its high power density and efficiency when operated in a combination of heat and power mode. In addition, the high operating temperature (650–1000 °C) of SOFC makes it easier when using hydrocarbon-based fuels. In SOFC, ceramic electrolytes are placed between two porous electrodes. Next, it is sandwiched between a pair of bipolar plates that act as cell houses. The performance of a single SOFC has been the focus of research over the past decade [10].

Recent studies have shown that SOFC control is challenging because of slow dynamics and operating limits. The main objective while SOFC is to supply active power demand, it is very important to operate fuel cells within the proper operating limits. To meet these requirements, an appropriate control strategy was developed in this study. This control strategy uses an optimal robust PI controller to control the active power of the plan and at the same time meets physical and operating constraints using two controllers obtained proportionally. The first is controlling the fuel utilization factor. The two controllers are the cathode anode pressure difference in such a way as to maintain the fuel utilization factor at an optimal value of 85 % and maintain the pressure difference between the anode and cathode within the 0–0.08 atm limit under transient conditions [11].

The SOFC cell stack model will be based on the following assumptions:

– gas is ideal;

– piles are fed with hydrogen and oxygen/air channels;

– channels that carry gas along the electrode have a fixed volume, small in length, so only need to determine one single pressure;

– the removal of each channel is through a single hole;

– the temperature is stable at all times;

– the only source of loss is ohmic;

– the Nernst equation can be applied.

According to the reference [12] relation to drainage characteristics of channels. A hole that is considered to be clogged, when fed with a mixture of average molar gas M (kg/kmol) and similar specific heat ratios, at a constant temperature, meets the following characteristics:

$$\frac{W}{P_U}=K\sqrt{M}, \tag{1}$$

where W is the mass flow, kg/s, K is the valve constant, √kmol kg/(atm s), P_U is the pressure in the channel.

For the case of the anode, the concept of using U_f fuels can be introduced. As a comparison between the flow of fuel that reacts and the flow of fuel that is injected into the stack. U_f is a way to express the molar fraction of water at discharge. According to this definition, equation (1) can be written as:

$$\frac{W_{an}}{P_{an}}=K_{an}\sqrt{\left(1-U_f\right)M_{H_2}+U_f M_{H_2O}}, \tag{2}$$

where W_{an} is the mass flow through the anode valve [kg/s]; K_{an} is the anode valve constant; M_{H_2}, M_{H_2O} is the molecular mass of hydrogen and water, each one is [kg/kmol]; P_{an} is the internal pressure in the anode channel [atm].

If it can be assumed that the molar flow of any gas through the valve is proportional to the partial pressure in the channel, the following can be stated:

$$\frac{q_{H_2}}{p_{H_2}}=\frac{K_{an}}{\sqrt{M_{H_2}}}=K_{H_2}, \tag{3}$$

$$\frac{q_{H_2O}}{p_{H_2O}}=\frac{K_{an}}{\sqrt{M_{H_2O}}}=K_{H_2O}, \tag{4}$$

where q_{H_2}, q_{H_2O} is the molar flow of hydrogen and water through the anode valve, kmol/s; p_{H_2}, p_{H_2O} is the partial pressure of hydrogen and water, atm; K_{H_2} is a molar constant of hydrogen and water valve.

Still according to the reference [12] for the output voltage from the stack is simple. Application of the Nernst equation and Ohm's law by considering ohmic losses, the output voltage of the stack is presented with the following statement:

$$V=N_0\left(E_0+\frac{RT}{2F}\left[\ln\frac{p_{H_2}p_{O_2}^{0.5}}{p_{H_2O}}\right]\right)-rI, \tag{5}$$

where E_0 is related to the free energy reaction (V); R is a universal gas constant, J/kmol K, r is ohmic losses (Ω).

Based on the references [13], it can be found that non-linear systems mainly originate from the Nernst equation:

$$V_0=N_0\left[E_0+\frac{R_0T_0}{2F_0}\ln\frac{p_{H_2}\left(p_{O_2}/101{,}325\right)^{0.5}}{P_{H_2O}}\right], \tag{6}$$

where partial pressure can be expressed as a transfer function,

$$p_{H_2}=\frac{1/K_{H_2}}{1+\tau_{H_2}s}\left(\frac{1}{1+\tau_f s}q_f-2K_rI\right), \tag{7}$$

$$p_{O_2}=\frac{1/K_{O_2}}{1+\tau_{O_2}s}\left(\frac{1/\tau_{H\text{-}O}}{1+\tau_f s}q_f-K_rI\right), \tag{8}$$

$$p_{H_2O} = \frac{1/K_{H_2O}}{1+\tau_{H_2O}s} 2K_r I. \quad (9)$$

The real output voltage can be reduced due to ohmic losses, activation, and concentration, which can be expressed as

$$V_{dc} = V_0 - n_{act} - n_{ohmic} - n_{conc}, \quad (10)$$

where,

$$n_{ohmic} = Ir, \quad (11)$$

$$n_{act} = \partial + \beta \ln I, \quad (12)$$

$$n_{conc} = -\frac{R_0 T_0}{2F_0} \ln\left(1 - \frac{I}{I_L}\right). \quad (13)$$

According to the reference [13], the average hydrogen flow rate for 384 cells is around 0.5–0.7 mol/s. If converted into liters/minute, for a flow rate of 0.5 mol/s to 1.200.6 L/min, then one cell needs a gas flow rate of about 1.75 L/min.

The above description shows that the performance of the SOFC cell stack is closely related to the fuel/oxygen channel. So optimizing fuel use is important to see the performance of each SOFC cell stack. This is also needed in making cell components, seals, and interconnections in SOFC systems.

$$\mathrm{Ar}_3(\mathrm{C}) \approx 910 - (310\mathrm{C}) - (80\mathrm{Mn}) - (80\mathrm{Mo}) - \\ -(55\mathrm{Ni}) - (20\mathrm{Cu}) - (15\mathrm{Cr}).$$

3. The aim and objectives of the study

This study aims to design a monitoring and regulation system for hydrogen/oxygen flow in the SOFC furnace operating environment based on the Arduino Mega 2560 microcontroller and computer interface.

To achieve this aim, the following objectives are accomplished:

– designing experimental set-ups for mechanics around the furnace, namely gas flow channels, gas flow valves, servo motors and sensor placement points;

– placing sensors as needed consisting of flow sensors, pressure sensors, hydrogen concentration sensors, voltage sensors and temperature sensors;

– designing electronic devices and sensor data acquisition based on a microcontroller;

– designing software algorithms on a microcontroller. So the system can monitor and regulate the gas flow valve. Furthermore, data can be stored and accessed by a computer.

4. Material and method of the research for experimental setup

The design of the experimental setup system in this study consists of three parts, namely: electronic devices, mechanical devices around the furnace and software. Electronic devices discuss about the electronic components used. These components include a microcontroller, servo motor controllers and sensor sensing systems.

The software is a microcontroller program that sends the rotation angle valve of the hydrogen/oxygen flow channel. The microcontroller also processes the data readings of each sensor. The results of data acquisition from the microcontroller can be seen and stored on a computer.

4. 1. Hardware Design

The hardware design consists of electronic and mechanical device blocks. The electronic device of this study uses the following components:

1) Arduino Mega2560 Microcontroller;
2) MG995 Servo Motor;
3) D6F-05N2-000 sensor;
4) HK1100C sensor;
5) MQ-8 sensor;
6) thermocouple K MAX6675;
7) voltage sensor (Op Amp).

All commercial components are arranged so that they become a system as shown in Fig. 4.

The mechanical device is a furnace with a maximum temperature of 1,000 degrees, a hydrogen/oxygen tank, a gas flow channel valve, sensors, servo motor, and a SOFC stack. Flow and pressure sensors are placed in the hydrogen/oxygen flow channel, as shown in Fig. 5.

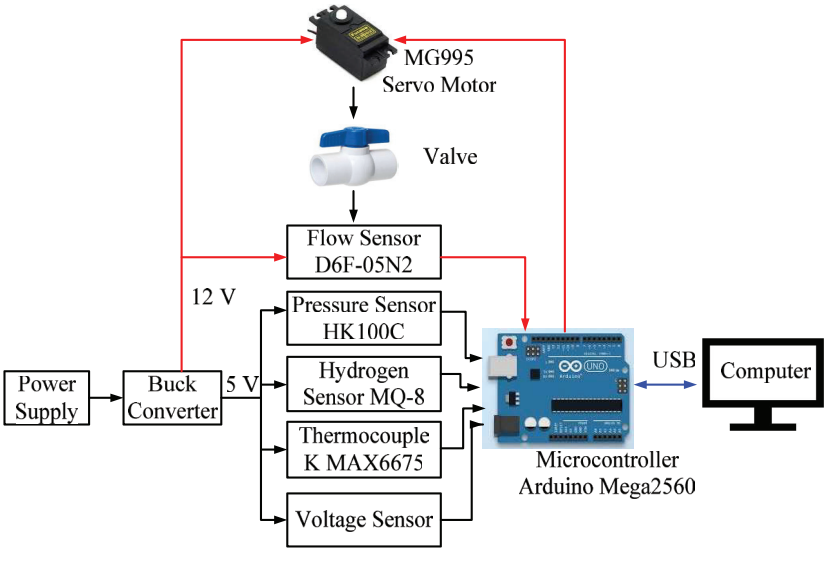

Fig. 4. Block regulating flow channel and sensor data acquisition

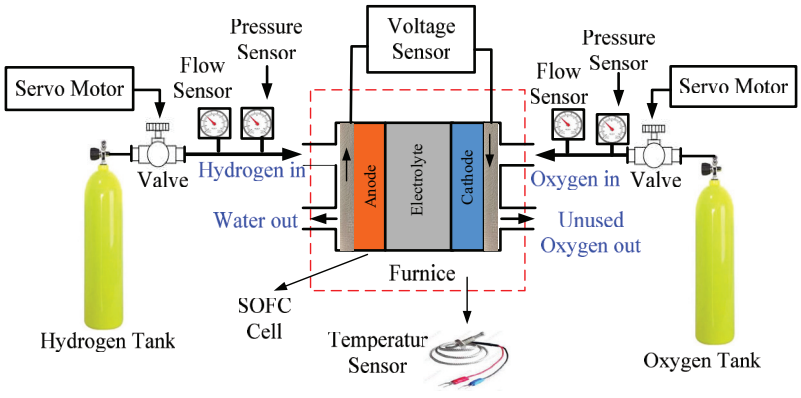

Fig. 5. SOFC experimental set-up mechanical block

Temperature sensors are placed in the furnace and voltage sensors are placed on the external wire collecting current. Then the hydrogen sensor is placed in the experimental chamber for the detection of excess hydrogen gas.

The SOFC spin cell design used is shown in Fig. 6. The cell has a diameter of 280 mm and a thickness of less than 1 mm. While the cell storage area is 220 mm in diameter, so that the cell can be placed and glued together by a seal.

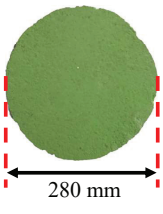

Fig. 6. SOFC single cell design

Cell storage area between the right and left can be removed because in the middle there is a locking sleeve. Overall storage of SOFC stacks has a length of 57 cm and 6 cm locking casings. Inside the locking sleeve, there is a cavity to hold a stack of SOFC cells, as shown in Fig. 7.

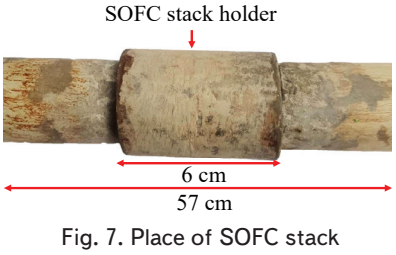

Fig. 7. Place of SOFC stack

4. 2. Software algorithm

Algorithm for software on a simple microcontroller. The concept is that all data collection and regulation processes of gas flow channel valves can be accessed through a computer. Data on the microcontroller can be stored and accessed by computers in real time. The flow diagram of the software algorithm in an electronic device system is shown in Fig. 8.

The initial process is the initialization of the sensor port, then the system will first read the hydrogen sensor to ensure that the room is safe from excessive hydrogen gas content. Furthermore, the process can be continued by entering the rotary angle value of the hydrogen/oxygen flow channel valve. The valve rotational angle value is adjusted to the requirements in the SOFC cell experiments. Thus, the system runs and all sensor outputs can be observed.

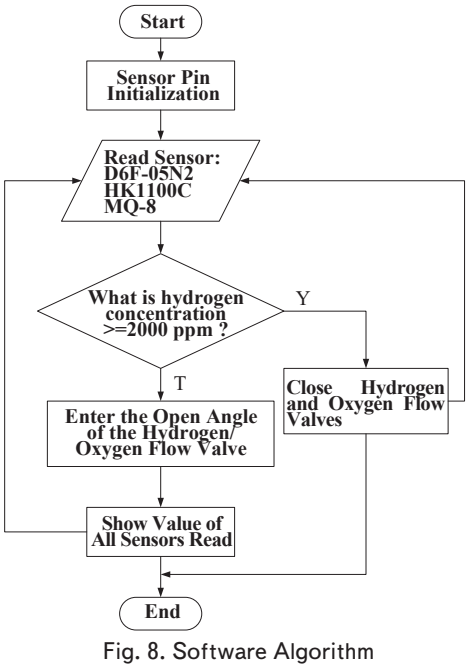

Fig. 8. Software Algorithm

5. Results of the research

5. 1. HK1100C Pressure Sensor Test

Testing the HK1100C sensor is done by flowing hydrogen and oxygen. Variations in the rotation angle of the gas flow channel valve are 10 to 90 degrees. The following are the results of the measurement and reading of the HK1100C sensor, shown in Fig. 9.

Based on Fig. 9, it can be concluded that the pressure sensor reading can detect the magnitude of changes in the hydrogen and oxygen systems.

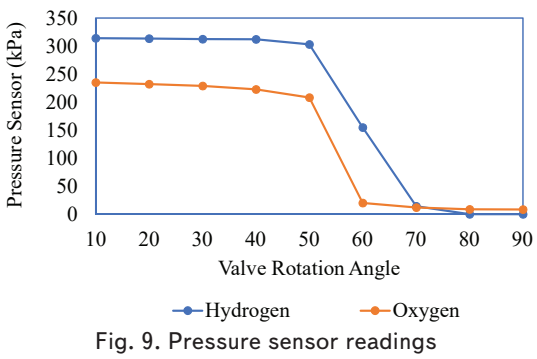

Fig. 9. Pressure sensor readings on the hydrogen/oxygen system

5. 2. D6F-05N2-000 Flow Sensor Test

Furthermore, the test is carried out with the angle of rotation of the hydrogen/oxygen flow channel valve. The channel valve is opened slowly from an angle of 10 (the valve closes) to 90 degrees (maximum opening). The flow of hydrogen/oxygen is regulated gradually through tank regulators ranging from 1, 2, 3, 4, and 5 liters/minute. The results are shown in Fig. 10, 11.

Fig. 10, 11 show the test results for each predetermined input variation. The valve rotation angle ranges within 10–90 degrees.

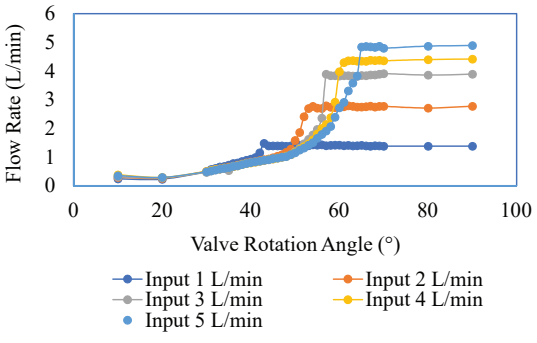

Fig. 10. Graph of relationship between valve rotation angle and oxygen flow

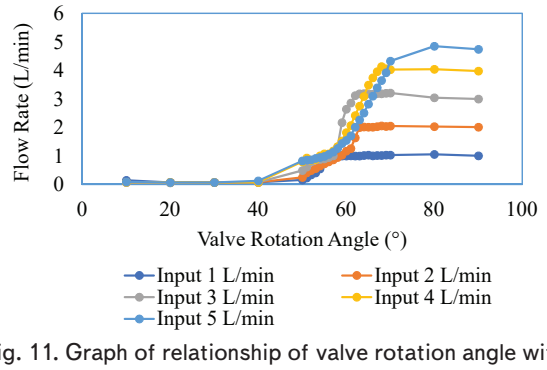

Fig. 11. Graph of relationship of valve rotation angle with hydrogen flow

Test results show that both the flow of hydrogen and oxygen are able to adjust according to input settings.

5. 3. Servo Motor Control Signal Test

The pulse width modulation (PWM) output signal is tested to determine the pulse width generated by the microcontroller for each rotation angle of the servo motor. Based on the test results using an oscilloscope, the period 1 wave PWM signal has a pulse width and variation as shown in Table 1. One of the PWM output signals at 20 ms is shown in Fig. 12, Table 1.

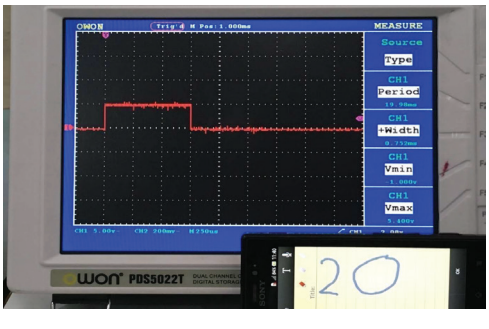

Fig. 12. Output Signal with PWM Value of 20

Table 1

Test PWM signal to adjust the rotation angle of the servo motor

PWM Value(ms)	Calculation		Measurement		Error	
	Pulse Width (ms)	Duty Cycle (%)	Pulse Width (ms)	Duty Cycle (%)	Pulse Width (ms)	Duty Cycle (%)
10	0.65	3.250	0.648	3.240	0.002	0.010
20	0.75	3.750	0.752	3.760	0.002	0.010
30	0.85	4.250	0.854	4.270	0.004	0.020
40	0.95	4.750	0.957	4.785	0.007	0.035
50	1.05	5.250	1.06	5.300	0.01	0.050
60	1.15	5.750	1.162	5.810	0.012	0.060
70	1.25	6.250	1.266	6.330	0.016	0.080
80	1.35	6.750	1.368	6.840	0.018	0.090
90	1.45	7.250	1.473	7.365	0.023	0.115
100	1.55	7.750	1.576	7.880	0.026	0.130
110	1.65	8.250	1.678	8.390	0.028	0.140
120	1.75	8.750	1.781	8.905	0.031	0.155
130	1.85	9.250	1,884	9.420	0.034	0.170
140	1.95	9.750	1.987	9.935	0.037	0.185
150	2.05	10.250	2.09	10.450	0.04	0.200
160	2.15	10.750	2.193	10.965	0.043	0.215
170	2.25	11.250	2.296	11.480	0.046	0.230

Fig. 12 shows the output PWM value of 20 produces a pulse width of 0.752 ms and a duty cycle of 3.76 %.

5. 4. Thermocouple sensor test

This sensor testing is carried out at room temperature. Thermocouple sensor type K MAX6675 is compared to a digital thermometer. Thermocouple sensor test results are shown in Table 2 below.

Table 2

Thermocouple sensor test results at room temperature

Thermometer	Thermocouple	Temperature Difference
28.1	28.5	0.4
28.5	29	0.5
28.5	28.5	0
28.5	28.75	0.25
28.5	28.75	0.25
28.5	28.75	0.25
28.5	28.5	0
28.1	28	0.1
28.1	28.75	0.65
28.1	28.5	0.4

Then the temperature sensor is tested at a temperature range of 100 by measuring the temperature at the boiling point of 100 °C water as shown in Table 3.

Thermocouple K MAX6675 sensor test is also performed on the furnace with samples taken every 100 °C increase. Initial measurements begin at room temperature to 800 °C as shown in Table 4.

Fig. 13 shows the thermocouple sensor measurement with the manual sensor on the furnace. The results show the linearity of both.

Table 3

Thermocouple sensor test results at the boiling point of water

Boiling Water	Thermocouple
100	110.7
100	111
100	99.5
100	98.75
100	97.5
100	95.5
100	94
100	93.5
100	92.25
100	91.25

Table 4

Comparison of thermocouple readings with furnace manual sensors

Set Point (°C)	Temperature		|error|	|%error|
	Manual Furnace (°C)	Thermocouple (°C)		
100	111.4	102.1	9.3	9.3
200	202.3	202	0.3	0.15
300	306	295.5	10.5	3.5
400	394.3	399.1	4.8	1.2
500	492.3	500.6	8.3	1.66
600	594	602.7	8.7	1.45
700	695.5	699.5	4	0.57
800	792.8	767.8	25	3.12

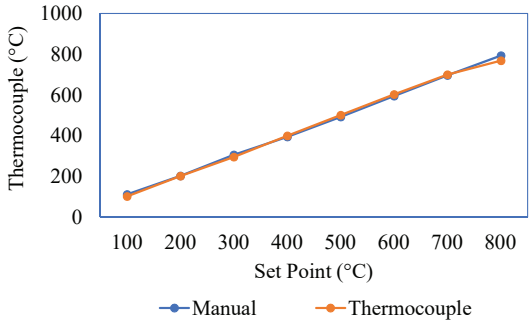

Fig. 13. Comparison of thermocouple with conventional temperature sensors

5. 5. Test of hydrogen and oxygen sensors

MQ-8 sensor is a sensor to determine the levels of hydrogen and oxygen in the air. To find out the changes in sensor values, measurements have been made in different places. Table 5 shows the results of measurements in normal air.

Table 5

MQ-8 sensor test results in normal air

ADC Value	Hydrogen Content (ppm)	Multimeter (volt)	Calculation (volt)	Voltage Difference
641	25	2	2	0
641	25	2.01	2	0.01
643	26	2.01	2.01	0
644	26	2.01	2.01	0
643	26	2	2.01	0.01
642	26	2	2	0
641	26	1.98	2	0.02
643	26	2	2.01	0.01
642	26	2	2	0
645	26	2	2.01	0.01

Table 6

MQ-8 sensor test results on water vapor

ADC Value	Hydrogen Content (ppm)	Multimeter (volt)	Calculation (volt)	Voltage Difference
630	2,503	3.08	3.07	0.01
634	2,514	3.10	3.09	0.01
638	2,531	3.12	3.11	0.01
638	2,530	3.12	3.11	0.01
634	2,514	3.10	3.09	0.01
640	2,538	3.13	3.12	0.01
644	2,554	3.15	3.14	0.01
658	2,610	3.22	3.21	0.01
664	2,630	3.25	3.24	0.01
695	2,772	3.41	3.39	0.02

Table 6 is the result of measurements on water vapor. From two measurements at different places, the concentration of hydrogen is not the same.

5. 6. Voltage Sensor Test

Voltage sensors are used to detect the output of a single cell stack of SOFC. For 1 SOFC cells ideally it has an output voltage range of 1 V [1]. So that for 1 cell SOFC has an output range between 0.1 to 1 V and the output current in the range of mA depends on the load used. The test results are shown in Table 7.

Table 7

Voltage sensor test results

Input (V)	Voltage (V)		|error|	|%error|
	Multimeter	Voltage Sensor		
0.1	0.1	0.1	0	0
0.2	0.2	0.2	0	0
0.3	0.3	0.3	0	0
0.4	0.4	0.4	0	0
0.5	0.5	0.5	0	0
0.6	0.62	0.62	0	0
0.7	0.71	0.71	0	0
0.8	0.8	0.79	0.01	1.25
0.9	0.9	0.89	0.01	1.11
1	1	0.99	0.01	1

The voltage sensor readings have a good response to the measured input. The difference between the two measurement tools is very small.

6. Discussion of experimental results

6. 1. HK1100C Pressure Sensor Test

HK1100C sensor shows a change in the value of the pressure is different from changes in the angle of rotation of the gas flow valve. When the valve closes (10 degrees), the maximum sensor read pressure and the output pressure entering the furnace are zero. Conversely, when

the pressure reads zero/small then the output pressure entering the furnace is large/maximum. Thus, the greater the valve rotation angle, the lower the sensor pressure value. From the above test, it can be concluded that the sensor can detect changes in pressure in both the hydrogen and oxygen systems, as shown in Fig. 9.

6. 2. D6F-05N2-000 flow sensor test

To see the performance of the D6F-05N2-000 sensor, the gas flow test is carried out as shown in Fig. 10. For the oxygen flow test, the angle of 10 degrees is the zero point or the position of the valve closure. At the position of the sensor valve closure issued a value of 0.24 L/min, so that the value of 0.24 becomes a correction factor. The test results showed the lowest D6F-05N2-000 sensor data was 0.24 L/min and the highest was 4.89 L/min. For the 10-degree hydrogen flow test, the zero point or valve closure position. The position of the hydrogen flow valve closure the sensor issuing a value of 0.07 L/min, so this 0.07 value becomes a correction factor. D6F-05N2-000 sensor data for hydrogen is the lowest 0.07 L/min and the highest is 4.74 L/min.

Thus, the D6F-05N2-000 sensor test results cannot detect exactly the zero value when the valve closes and vice versa at the maximum opening does not read exactly at the value of 5 L/min.

6. 3. Servo motor signal test

Servo motors are used to open hydrogen/oxygen flow valves. The method used is pulse width modulation (PWM). This PWM signal is given by the microcontroller by regulating the duty cycle. Based on Table 1, the average pulse width error that occurs is 0.022 ms. The average error duty cycle that occurs is 0.111 %. These results prove that the PWM output from the microcontroller is appropriate. Fig. 12 shows one of the 20 ms PWM outputs producing 0.752 ms pulse width and 3.76 % duty cycle.

6. 4. Thermocouple sensor test

The thermocouple sensor used is type K MAX6675. The sensor is tested starting from room temperature to a temperature of 850 degrees. The data in Table 2 is taken based on the set points given. Eight K MAX6675 thermocouple sensor data are compared with conventional furnace temperature sensor meters. Between the conventional temperature sensor and K MAX6675 there is a difference in value. This is possible because the sensor material factors are not the same. Overall, the average error that occurs can reach 2.6 %. Thus, this thermocouple sensor can be used in this system.

In boiling water, the average temperature of the test results was 98.75 °C. Based on the test results, it can be seen that the longer the temperature decreases. This is caused by testing the boiling point of water carried out indoors so that there is an adjustment of water temperature with room temperature. While at room temperature can be seen according to Table 2. The temperature reading by the thermocouple sensor is in accordance with an average error of 0.28 %.

6. 5. Hydrogen level sensor test

The hydrogen level sensor is used to detect hydrogen leakage or excess in the experimental room. Then the sensor test is based on changes in different conditions. The hydrogen sensor is tested in normal air and in water vapor. Based on Tables 5, 6, it can be seen that from the data taken. Sensor data shows changes in normal conditions. Thus, the commercial sensor can be applied to this device system.

It can be seen that there is a relatively small difference in the measurement of the sensor voltage which is 0.008 volts in normal air and 0.011 volts in water vapor. Thus, it can be said that the reading of the ADC value, which is subsequently converted to a voltage value is functional. The average hydrogen level detected by the sensor under normal air conditions is 2288 ppm and water vapor is 3043 ppm.

6. 6. Voltage Sensor Testing

If losses on SOFC cells are ignored, the ideal DC voltage output generated from a SOFC cell is in the range of 1 V [1]. Thus, the required voltage sensor on the external wire section with a minimum accuracy is 0.1 V. Based on the tests in Table 7, the sensor response already has the ability in accordance with system requirements. The maximum range of the voltage sensor is adjustable according to system requirements.

6. 7. Realization of Electronic and Mechanical Devices

In realizing the experimental setup system to see SOFC's single cell performance. This system is applied to simple furnaces with a maximum combustion temperature of 1000 degrees. The fuel used is hydrogen and the air substitute uses oxygen. Hydrogen and oxygen are supplying fuel/air needs at the electrodes (anode and cathode). To realize the device as a whole, several manufacturing stages are carried out. The first is the layout of the PCB board for the placement of components and sensors, shown in Fig. 14. The second is the mechanical design of the hydrogen and oxygen channels, shown in Fig. 15. The third is the design for the cell and place of the SOFC cell stack in the furnace, shown in Fig. 6, 7, 16.

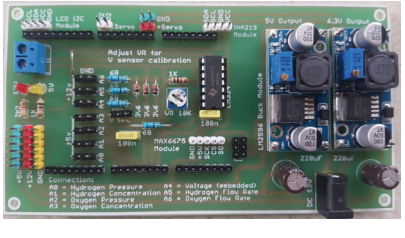

Fig. 14. Realization of electronic device models

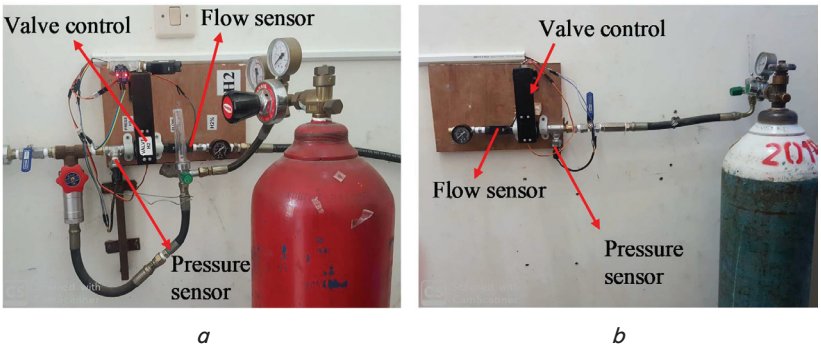

a *b*

Fig. 15. Realization of mechanical systems on hydrogen and oxygen tanks: *a* — Hydrogen tank mechanic; *b* — Oxygen tank mechanic

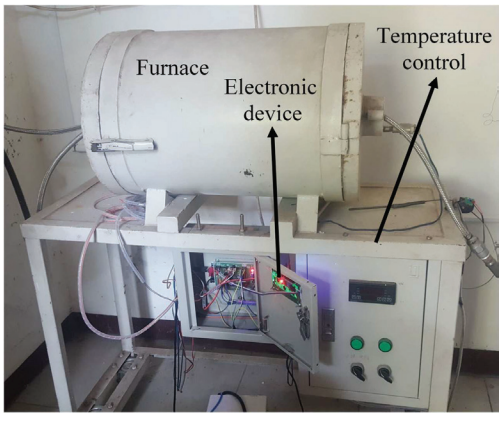

Fig. 16. Realization of the placement of electronic devices in the furnace

To realize the device as a whole, several stages of production are carried out. The first is the layout of the PCB board for the placement of components and sensors, shown in Fig. 14. The second is the mechanical design of hydrogen channels and oxygen channels, shown in Fig. 15. The third is the design for cells and placing a stack of SOFC cells in the furnace, shown in Fig. 6, 7, 16.

For further research, a direction can be developed towards the number of SOFC cell stacks that can be put into the furnace. Further research can also be directed as a simple SOFC system module as an alternative power source.

7. Conclusions

1. This research focuses on making sensor data acquisition and control systems for hydrogen and oxygen flow valves. The flow angle of the valve can be adjusted according to the needs and use on a laboratory scale.

2. Based on the D6F-05N2 sensor test, the measured flow value for oxygen is between 0.24 to 4.89 L/min and hydrogen 0.07 to 4.74 L/min. Comparison between oxygen and hydrogen tank regulator meters obtained flow with an average error of 0.09 and 0.122.

3. HK1100C sensor test was detected at the valve opening of 10 degrees, hydrogen pressure of 312.93 kPa and oxygen of 235.14 kPa. This condition is the maximum pressure.

4. The temperature sensor has an average error of 2.6 % and the voltage sensor has an accuracy of up to 0.1 V. For hydrogen sensors can follow changes in the concentration of hydrogen in the air. The relatively small difference in measurement of sensor voltage is 0.008 volts in normal air and 0.011 volts in water vapor.

Acknowledgments

The author would like to thank Sulistyo, Aris Triwiyatno for his guidance. Also thanks to DRPM Dikti for providing research grants.

References

1. Vielstich, W., Lamm, A., Gasteiger, H. A., Yokokawa, H. (Eds.) (2010). Handbook of Fuel Cells. Fundamental Technology and Applications. John Wiley & Sons. doi: https://doi.org/10.1002/9780470974001
2. Wang, C. (2006). Modeling and Control of Hybrid. Theses Diss. Mont. State Univ., 13 (5), 399–419.
3. Canavar, M., Kaplan, Y. (2015). Effects of mesh and interconnector design on solid oxide fuel cell performance. International Journal of Hydrogen Energy, 40 (24), 7829–7834. doi: https://doi.org/10.1016/j.ijhydene.2014.11.101
4. Guk, E., Kim, J.-S., Ranaweera, M., Venkatesan, V., Jackson, L. (2018). In-situ monitoring of temperature distribution in operating solid oxide fuel cell cathode using proprietary sensory techniques versus commercial thermocouples. Applied Energy, 230, 551–562. doi: https://doi.org/10.1016/j.apenergy.2018.08.120
5. Darjat, Sulistyo, Triwiyatno, Sudjadi, Kurniahadi (2020). Designing Hydrogen and Oxygen Flow Rate Control on a Solid Oxide Fuel Cell Simulator Using the Fuzzy Logic Control Method. Processes, 8 (2), 154. doi: https://doi.org/10.3390/pr8020154
6. Zhu, Y., Tomsovic, K. (2002). Development of models for analyzing the load-following performance of microturbines and fuel cells. Electric Power Systems Research, 62 (1), 1–11. doi: https://doi.org/10.1016/s0378-7796(02)00033-0
7. Wincewicz, K., Cooper, J. (2005). Taxonomies of SOFC material and manufacturing alternatives. Journal of Power Sources, 140 (2), 280–296. doi: https://doi.org/10.1016/j.jpowsour.2004.08.032
8. Sun, C., Stimming, U. (2007). Recent anode advances in solid oxide fuel cells. Journal of Power Sources, 171 (2), 247–260. doi: https://doi.org/10.1016/j.jpowsour.2007.06.086
9. Mahato, N., Banerjee, A., Gupta, A., Omar, S., Balani, K. (2015). Progress in material selection for solid oxide fuel cell technology: A review. Progress in Materials Science, 72, 141–337. doi: https://doi.org/10.1016/j.pmatsci.2015.01.001
10. Dey, T., Singdeo, D., Bose, M., Basu, R. N., Ghosh, P. C. (2013). Study of contact resistance at the electrode–interconnect interfaces in planar type Solid Oxide Fuel Cells. Journal of Power Sources, 233, 290–298. doi: https://doi.org/10.1016/j.jpowsour.2013.01.111
11. Taher, S. A., Mansouri, S. (2014). Optimal PI controller design for active power in grid-connected SOFC DG system. International Journal of Electrical Power & Energy Systems, 60, 268–274. doi: https://doi.org/10.1016/j.ijepes.2014.02.010
12. Padullés, J., Ault, G. W., McDonald, J. R. (2000). An integrated SOFC plant dynamic model for power systems simulation. Journal of Power Sources, 86 (1-2), 495–500. doi: https://doi.org/10.1016/s0378-7753(99)00430-9
13. Sun, L., Li, D., Wu, G., Lee, K. Y., Xue, Y. (2015). A Practical Compound Controller Design for Solid Oxide Fuel Cells. IFAC-PapersOnLine, 48 (30), 445–449. doi: https://doi.org/10.1016/j.ifacol.2015.12.419